# FIRST-FORBIDDEN $\Delta J = 0$ , $\pm 2~\beta$ -DECAYS WITHIN A SELF-CONSISTENT EFFECTIVE POTENTIAL

S. Ünlü 🗅

Department of Physics, Burdur Mehmet Akif Ersoy University, Burdur, Turkey

H. BİRCAN

Department of Physics, Kütahya Dumlupınar University, Kütahya, Turkey

N. Cakmak

Department of Physics, Karabük University, Karabük, Turkey

Received 30 April 2025, accepted 28 July 2025, published online 22 August 2025

The first-forbidden  $\Delta J=0,\,\pm 2$  transitions are analyzed by using a self-consistent effective potential within the framework of proton–neutron quasi-particle random phase approximation (pn-QRPA) method. The self-consistency arises from the fact that the particle–hole and particle–particle strength parameters can be found analytically within the present approximation. The beta ( $\beta$ ) decay matrix elements and  $\log ft$  values are computed and compared with the corresponding experimental data. The present approximation is usually successful in reproducing the experimental data.

DOI:10.5506/APhysPolB.56.9-A2

## 1. Introduction

It is well known that charge-exchange spin-spin (Gamow-Teller) transitions play a significant role in understanding the nuclear structure. For medium-heavy and heavy nuclei, the first-forbidden transitions become more important than the Gamow-Teller (GT) transitions.

In our opinion, the literature related to the weak interaction processes needs more experimental and theoretical results concerning the first-forbidden transitions. The  $\beta$ -decay strength for the transitions between the initial and final ground states was calculated for both the allowed and first-forbidden cases [1]. In this work, the  $\beta$ -decay properties of odd–odd nuclei to the excited states of the neighboring even–even nuclei were defined using the QRPA method. The first-forbidden beta transitions for  $\Delta J=0$ ,  $\pm 2$  were studied using the RPA method for two different quasi-particle

excitations [2]. Here, the relativistic  $\beta$ -moment was assumed to be proportional to the matrix element of the non-relativistic one. For  $\Delta J = 0$ transitions, the calculated ft values show a good consistency with the corresponding experimental values. For the unique first-forbidden transitions  $(\Delta J = \pm 2)$ , the re-normalization effects improved the theoretical values. The unique first-forbidden (U1F) transitions were calculated within the pn-QRPA method [3, 4]. The calculations clearly proved the effect of the U1F transitions on the total transition strength [3]. The pn-QRPA method was modified to calculate the U1F decay rates in stellar matter [5]. The QRPA studies based on the Fayans energy functional theory were extended for a consistent treatment of the allowed and first-forbidden contributions to rprocess half-lives [6]. It was clearly seen that the dominant contribution to the total decay half-life comes from the first-forbidden transitions, mostly for the nuclei having closed shells. The half-lives for r-process waiting-point nuclei were calculated within a large-scale shell model (LSSM) considering first-forbidden contributions [7].

The pn-QRPA method was used to study  $0^+ \leftrightarrow 0^-$  beta transitions for 90 < A < 214 nuclei [8]. The calculated results are in good consistency with the corresponding experimental data. The  $\beta$ -decay half-lives of N=126 isotones were calculated by considering both the Gamow-Teller and first-forbidden transitions within the shell model [9]. It was shown that the consideration of the first-forbidden contributions leads to a remarkable reduction in the decay half-lives. The relativistic version of the pn-QRPA method was used to obtain the  $\beta$ -decay half-lives and  $\beta$ -delayed neutron emission probabilities for many nuclei [10]. The calculated results showed that the first-forbidden transitions make a significant contribution to the total decay probability. The allowed and unique first-forbidden transitions for both spherical and deformed nuclei were calculated within the pn-QRPA method with a schematic separable interaction [11]. The inclusion of the first-forbidden contributions ensures a reliable comparison between the calculated and experimental  $\beta$ -decay half-lives. The influences of the quenching of the weak axial-vector coupling constant on the Gamow-Teller and forbidden  $\beta$ -decays were investigated [12]. The LSSM calculations incorporate different quenching values ranging from 0.38 to 1.266 [7]. The first-forbidden  $\beta$ -decay log ft values for Z = (82-126) and N = (126-184) nuclei were studied using the shell model [13].

In the present work, the first-forbidden  $\Delta J=0,\pm 2$  transitions are calculated by using Pyatov's restoration procedure in the framework of the pn-QRPA method. The  $\beta$ -decay properties are defined without using any adjustable interaction parameter. The calculated  $\beta$ -decay quantities within the present approximation usually show good agreement with the corresponding experimental data. We divide our script into four sections. The mathematical procedure related to our calculations is described in Section 2.

Our calculated results and their comparison with the previous theoretical and measured data are presented in Section 3. Conclusions are stated in Section 4.

#### 2. Method

#### 2.1. Motivation

The theoretical investigations on charge-exchange collective excitations in nuclei are usually performed using approximations that contain at least one free parameter. However, there are some self-consistent approximations to define  $\beta$ -decay properties [10, 14–16]. Surely, these self-consistent approximations make important contributions to the theoretical explanation of  $\beta$ -decay properties. Nevertheless, they contain a fitting procedure to obtain the decay properties. At this point, we try to define  $\beta$ -decay properties without any fitting procedure by means of Pyatov's restoration method.

Pyatov's restoration method is an effective way to study the charge-exchange collective vibrations in nuclei without using any adjustable parameter [17]. According to this method, the strength parameter of the effective interaction potential can be determined from a commutator correlation between the Hamiltonian operator and the decay operator. The corresponding commutator correlation for super-allowed Fermi transitions is defined as follows:

$$\left[\hat{H} - \hat{V}_{\mathrm{C}}, \hat{\tau}_{\rho}\right] = 0 \,,$$

where  $\hat{H}$ ,  $\hat{V}_{\rm C}$ , and  $\hat{\tau}_{\rho}$  ( $\rho=\pm$ ) are the operator representations for the total Hamiltonian, Coulomb potential, and raising (+) or lowering (-) isospin, respectively. The decay operator for the allowed Gamow–Teller transitions can commute with the central part of the nuclear Hamiltonian as

$$\left[ \hat{H} - \hat{V}_{\mathrm{C}} - \hat{V}_{ls}, \hat{\sigma}_{\eta} \hat{\tau}_{\rho} \right] = 0,$$

where  $\hat{V}_{ls}$  is the operator representation for spin-orbit potential and  $\hat{\sigma}_{\eta}(\eta = 0, \pm 1)$  is the Pauli spin operator.

The above commutator conditions are violated in the mean-field level of approximation. Then, Pyatov's method can be used to restore these violations in the commutator conditions. Thus, the super-allowed (Fermi) and allowed spin—isospin (Gamow—Teller) transitions have been investigated using this method and the experimental data have been successfully reproduced [18–28].

Investigation of the weak interaction processes also makes a serious contribution to the explanation of the astrophysical processes such as nuclear synthesis [29] and supernova explosions [6, 30]. Especially, a correct definition of  $\beta$ -decay properties for neutron-rich nuclei plays a key role in r-process

investigations. For neutron-rich nuclei, the first-forbidden transitions are favored mainly due to the phase-space amplification for these transitions. Hence, the determination of the first-forbidden decay properties as being free of the effective interaction strength parameter becomes a prominent issue.

The corresponding decay operator for the first-forbidden transitions does not commute with the total nucleus Hamiltonian due to the Coulomb, spinorbit, and kinetic energy terms

$$\left[\hat{H} - \hat{V}_{\rm C} - \hat{V}_{ls} - \hat{P}^2/2m, r\left(\hat{Y}_1 \otimes \hat{\sigma}\right)_{\lambda} \hat{\tau}_{\rho}\right] = 0, \qquad (\lambda = 0, 1, 2),$$

where  $\hat{P}$  is a linear momentum operator. This commutator condition is broken in the mean-field (MF) approximation as follows:

$$\left[\hat{H}_{\mathrm{MF}} - \hat{V}_{\mathrm{C}} - \hat{V}_{ls} - \hat{P}^{2}/2m, r\left(\hat{Y}_{1} \otimes \hat{\sigma}\right)_{\lambda} \hat{\tau}_{\rho}\right] \neq 0.$$

At this point, the nucleon–nucleon effective interaction potential can be added in such a way that the broken commutator condition is restored

$$\left[\hat{H}_{\mathrm{MF}} + \hat{h} - \hat{V}_{\mathrm{C}} - \hat{V}_{ls} - \hat{P}^{2}/2m, r\left(\hat{Y}_{1} \otimes \hat{\sigma}\right)_{\lambda} \hat{\tau}_{\rho}\right] = 0.$$

Thus, the strength constant of the effective interaction potential can be determined from this commutator condition. A summary of the mathematical procedure is given in the next subsection. The detailed formalism related to the restoration of the broken commutator condition is available in [31].

## 2.2. Mathematical procedure

The single quasi-particle Hamiltonian for a system of nucleons in a spherical symmetric average field with pairing forces is given by

$$\hat{H}_{\text{sqp}} = \sum_{jm} \varepsilon_j(\tau) \,\hat{\alpha}_{jm}^{\dagger}(\tau) \,\hat{\alpha}_{jm}(\tau) , \qquad \tau = n, p, \qquad (1)$$

where  $\hat{\alpha}_{jm}^{\dagger}$  and  $\hat{\alpha}_{jm}$  are one quasi-particle creation and annihilation operators, respectively. The pairing forces between nucleons are included utilizing Bogolyubov's quasi-particle transformations [32].

The commutator correlation between charge-exchange spin—dipole and Hamiltonian operators is broken in the single quasi-particle level of approximation as follows:

$$\left[ \hat{H}_{\text{sqp}} - \hat{V}_{\text{C}} - \hat{V}_{ls} - \hat{P}^2 / 2m, \hat{F}_{\lambda\mu}^{\rho} \right] \neq 0.$$
 (2)

Here,  $\hat{F}^{\rho}_{\lambda\mu}$  is the charge-exchange spin–dipole operator consisting of a combination of  $\beta^+$  and  $\beta^-$  decay operators in the following form:

$$\hat{F}^{\rho}_{\lambda\mu} = \frac{1}{2} \left( \hat{T}^{+}_{\lambda\mu} + \rho (-1)^{\lambda+\mu} \hat{T}^{-}_{\lambda,-\mu} \right) , \qquad \rho = \pm .$$
 (3)

The  $\beta^{(\pm)}$  decay operators are defined as

$$\hat{T}_{\lambda\mu}^{+} = \sum_{np} \bar{b}_{np}(\lambda) \hat{C}_{np}^{\dagger}(\lambda\mu) + (-1)^{\lambda+\mu+1} b_{np}(\lambda) \hat{C}_{np}(\lambda, -\mu) ,$$

$$\hat{T}_{\lambda\mu}^{-} = \left(\hat{T}_{\lambda\mu}^{+}\right)^{\dagger} ,$$

where  $\hat{C}_{np}^{\dagger}(\lambda\mu)(\hat{C}_{np}(\lambda\mu))$  is one quasi-boson creation (annihilation) operator,  $\lambda$  and  $\mu$  are the corresponding nuclear spin ( $\lambda^{\pi}=0^{-}$  or  $2^{-}$ ) for the transition and its projection, respectively. The reduced matrix elements are given as

$$\bar{b}_{np}(\lambda) = \frac{\left\langle j_n \left| \left| \left[ r \left( \hat{Y}_1 \otimes \hat{\sigma} \right) \right]_{\lambda \mu} \right| \right| j_p \right\rangle}{\sqrt{(2\lambda + 1)}} u_n v_p,$$

$$b_{np}(\lambda) = \frac{\bar{b}_{np}(\lambda)}{u_n v_p} u_p v_n,$$

where v and u are single-particle and hole amplitudes, respectively.

The remaining part of the single quasi-particle Hamiltonian, besides the Coulomb, spin-orbit, and kinetic energy terms, consists of iso-scalar and iso-vector terms. The iso-vector term  $(V_1)$  causes the commutator correlation to be violated

$$\left[\hat{V}_1, \hat{F}^{\rho}_{\lambda\mu}\right] \neq 0. \tag{4}$$

Hence, the nucleon–nucleon effective interaction potential should be considered in such a way that the broken commutator correlation is restored

$$\left[\hat{V}_1 + \hat{h}, \hat{F}^{\rho}_{\lambda\mu}\right] = 0. \tag{5}$$

The effective interaction potential consists of particle-hole (ph) and particle-particle (pp) terms and is defined within Pyatov's restoration method

$$\hat{h} = \sum_{\rho} \frac{1}{4\gamma_{\rm ph}^{\rho}} \sum_{\mu} \left[ \hat{V}_{1}, \hat{F}_{\lambda\mu}^{\rho} \right]_{\rm ph}^{\dagger} \cdot \left[ \hat{V}_{1}, \hat{F}_{\lambda\mu}^{\rho} \right]_{\rm ph} + \sum_{\rho} \frac{1}{4\gamma_{\rm pp}^{\rho}} \sum_{\mu} \left[ \hat{V}_{1}, \hat{F}_{\lambda\mu}^{\rho} \right]_{\rm pp}^{\dagger} \cdot \left[ \hat{V}_{1}, \hat{F}_{\lambda\mu}^{\rho} \right]_{\rm pp} .$$
 (6)

As seen in Eq. (6), the commutator correlation in Eq. (5) contains two unknown strength parameters. Therefore, the particle—hole  $(\gamma_{\rm ph}^{\rho})$  and particle—particle  $(\gamma_{\rm pp}^{\rho})$  strength parameters can be determined analytically from two different commutator correlations as follows:

$$\left[\frac{1}{2}\hat{V}_1 + \hat{h}_{\rm ph}, \hat{F}^{\rho}_{\lambda\mu}\right] = 0, \qquad (7)$$

$$\left[\frac{1}{2}\hat{V}_1 + \hat{h}_{pp}, \hat{F}^{\rho}_{\lambda\mu}\right] = 0, \qquad (8)$$

$$\hat{h}_{\rm ph} = \sum_{\rho} \frac{1}{4\gamma_{\rm ph}^{\rho}} \sum_{\mu} \left[ \hat{V}_{1}, \hat{F}_{\lambda\mu}^{\rho} \right]_{\rm ph}^{\dagger} \cdot \left[ \hat{V}_{1}, \hat{F}_{\lambda\mu}^{\rho} \right]_{\rm ph} \,,$$

$$\hat{h}_{\rm pp} = \sum_{\rho} \frac{1}{4\gamma_{\rm pp}^{\rho}} \sum_{\mu} \left[ \hat{V}_{1}, \hat{F}_{\lambda\mu}^{\rho} \right]_{\rm pp}^{\dagger} \cdot \left[ \hat{V}_{1}, \hat{F}_{\lambda\mu}^{\rho} \right]_{\rm pp}^{\rho}.$$

The following expressions for particle—hole and particle—particle strength parameters are found using the commutator correlations in Eqs. (7) and (8), respectively,

$$\gamma_{\rm ph}^{\rho} = \rho(-1)^{\lambda+\mu} \left\langle 0 \left| \left[ \left[ \hat{V}_1, \hat{F}_{\lambda,-\mu}^{\rho} \right]_{\rm ph}, \hat{F}_{\lambda\mu}^{\rho} \right] \right| 0 \right\rangle, \tag{9}$$

$$\gamma_{\rm pp}^{\rho} = \rho(-1)^{\lambda+\mu} \left\langle 0 \left| \left[ \left[ \hat{V}_1, \hat{F}_{\lambda,-\mu}^{\rho} \right]_{\rm pp}, \hat{F}_{\lambda\mu}^{\rho} \right] \right| 0 \right\rangle. \tag{10}$$

The collective Hamiltonian for the first-forbidden transitions can be defined as follows:

$$\hat{H} = \hat{H}_{\text{sqp}} + \hat{h} \,. \tag{11}$$

The following equation is solved to determine the corresponding energies and wave functions for the first-forbidden excitations in the neighboring odd-odd nuclei

$$\left[\hat{H}, \hat{Q}_i^{\dagger} (\lambda \mu)\right] |0\rangle = \omega_i \hat{Q}_i^{\dagger} (\lambda \mu) |0\rangle. \tag{12}$$

The first-forbidden excitations in odd-odd nuclei are represented by a phonon-creation operator in the following form:

$$\hat{Q}_{i}^{\dagger}(\lambda\mu)|0\rangle = \sum_{np} \psi_{np}^{i} \hat{C}_{np}^{\dagger}(\lambda\mu) + (-1)^{\lambda+\mu} \varphi_{np}^{i} \hat{C}_{np}(\lambda, -\mu).$$
 (13)

Generally, the  $\beta$ -decay probabilities are given by the following formula:

$$B(\lambda_{i} \to \lambda_{f}) = \frac{1}{2\lambda_{i} + 1} \left| M_{\beta^{\pm}} \left( \lambda_{i} \to \lambda_{f}, \mu \right) \right|^{2}. \tag{14}$$

The  $\beta$ -decay matrix elements are usually defined as follows:

$$M_{\beta^{\pm}}(\lambda_{\rm i} \to \lambda_{\rm f}, \mu) = \left\langle \lambda_{\rm f} \left| \hat{T}_{\lambda\mu}^{\pm} \right| \lambda_{\rm i} \right\rangle.$$
 (15)

The decay rates for the first-forbidden  $\Delta J = 0, \pm 2$  transitions are given by the following expressions [33]:

$$ft(\lambda = 0) = \frac{D}{(g_{\rm A}/g_{\rm V})^2 4\pi B(\lambda_{\rm i} \to \lambda_{\rm f}, \ \lambda = 0)}$$
(16)

$$ft(\lambda = 2) = \frac{3}{4} \frac{D}{(g_{\rm A}/g_{\rm V})^2 4\pi B(\lambda_{\rm i} \to \lambda_{\rm f}, \ \lambda = 2)}$$
 (17)

with

$$B(\lambda_{i} \to \lambda_{f}, \lambda = 0) = \frac{1}{2\lambda_{i} + 1} \times \left\langle \lambda_{f} \left\| \pm M(\lambda = 0) - i \frac{m_{e}c}{\hbar} \xi M(\kappa = 1, \lambda = 0) \right\| \lambda_{i} \right\rangle^{2},$$
(18)

$$B(\lambda_{\rm i} \to \lambda_{\rm f}, \lambda = 2) = \frac{1}{2\lambda_{\rm i} + 1} \left\langle \lambda_{\rm f} \middle\| M^{\pm} \left( \kappa = 1, \lambda = 2, \mu \right) \middle\| \lambda_{\rm i} \right\rangle^2, \tag{19}$$

where the constants are taken as D=6250 sec,  $g_{\rm A}/g_{\rm V}=-1.24$  [34]. The decay matrix elements for  $\Delta J=0$  transitions are calculated within the  $\xi$ -approximation. According to this approximation, the Coulomb energy may be represented by the dimensionless parameter

$$\xi \equiv \frac{Ze^2}{2R} \frac{1}{m_e c^2} \approx 1.2ZA^{-1/3}$$
,

where the Coulomb radius is taken as  $R \approx 1.2 A^{1/3}$  and the conditions are defined as  $\xi \gg \frac{Q}{m_e c^2}$  and  $\xi \gg 1$ . In the  $\xi$ -approximation, the terms of relative order  $\xi^{-1} Q/m_e c^2$  and  $\xi^{-1}$  are neglected.

The  $\beta$ -decay multipole operators are given as

$$M(\lambda = 0) = \frac{1}{\sqrt{4\pi}c} \sum_{k} \hat{t}_{\pm}(k) (\vec{\sigma_k} \cdot \vec{v_k}) ,$$

$$M(\kappa = 1, \lambda = 0) = \sum_{k} \hat{t}_{\pm}(k) r_k (Y_1(\hat{r}_k) \sigma_k)_0 ,$$

$$M(\kappa = 1, \lambda = 2, \mu) = \sum_{k} \hat{t}_{\pm}(k) r_k (Y_1(\hat{r}_k) \sigma_k)_{\mu} .$$

#### 3. Results and discussions

The calculated results related to the first-forbidden  $\Delta J = 0$ ,  $\pm 2$  transitions are presented in this section. The Woods–Saxon potential with the Chepurnov parametrization is used to define a single-particle basis [35]. The proton and neutron pairing gaps are defined as  $\Delta_p = C_p/\sqrt{A}$  and  $\Delta_n = C_n/\sqrt{A}$ , respectively [33]. The pairing strength parameters ( $C_p$  and  $C_n$ ) are fixed so that the experimental pairing gaps [36] are reproduced.

## 3.1. Matrix elements for $\Delta J = 0$ transitions

The charge-exchange  $0^- \leftrightarrow 0^+$  transition probabilities are computed by using the  $\xi$ -approximation [33] in which the decay amplitude consists of relativistic and non-relativistic terms as seen in Eq. (18). Table 1 shows the values of the  $\xi$  parameter and Q energies for the nuclei under consideration. The calculated values for the relativistic and non-relativistic contributions are shown in Table 2. Also, a comparison of the calculated non-relativistic matrix elements with the correlated RPA results [2] and the corresponding experimental data [37] is given for a total of 10 nuclei with the mass range of  $96 \le A \le 214$ .

Table 1. The values of the  $\xi$  parameter and decay energies for  $\Delta J = 0$  transitions.

Transition	Q [MeV]	ξ
${}^{96}Y(0^{-}) \rightarrow {}^{96}Zr(0^{+})$	7.096	10.22
$^{120}{\rm Xe}(0^+) \rightarrow \ ^{120}{\rm I}(0^-)$	1.870	13.14
$^{140} \mathrm{Ba}(0^{+}) \rightarrow ^{140} \mathrm{La}(0^{-})$	0.466	12.94
$^{144}{\rm Ce}(0^+) \rightarrow \ ^{144}{\rm Pr}(0^-)$	) 0.319	13.28
$^{144} Pr(0^{-}) \rightarrow ^{144} Nd(0^{+})$	(2.998)	13.51
$^{206} \mathrm{Hg}(0^{+}) \rightarrow ^{206} \mathrm{Tl}(0^{-})$	) 1.308	16.25
$^{206}\text{Tl}(0^{-}) \rightarrow ^{206}\text{Pb}(0^{+})$	1.532	16.46
$^{210}\text{Pb}(0^+) \rightarrow ^{210}\text{Bi}(0^-)$	0.017	16.55
$^{212}\text{Pb}(0^+) \rightarrow ^{212}\text{Bi}(0^-)$	0.331	16.50
$^{214}\text{Pb}(0^+) \rightarrow ^{214}\text{Bi}(0^-)$	0.666	16.45

The correlated RPA results given in the fifth column of Table 2 were obtained using a separable residual interaction potential, which contains an adjustable parameter. The reduced matrix elements in the last column are extracted from experimental log ft values [37]. For the  $^{140}$ Ba  $\rightarrow$   $^{140}$ La,  $^{144}$ Pr  $\rightarrow$   $^{144}$ Nd, and  $^{144}$ Ce  $\rightarrow$   $^{144}$ Pr transitions, the present matrix elements are in

Table 2. Calculated values of relativistic and non-relativistic matrix elements within the  $\xi$ -approximation for  $\Delta J=0$  transitions. The present non-relativistic matrix elements can be compared with the correlated RPA results and the corresponding experimental data. The  $2^{\rm nd}$  column shows the calculated energies of the  $0^-$  states in odd–odd nuclei.

Transition	Energy	$M(\lambda = 0)$	$M(\kappa = 1, \lambda = 0)$	RPA [2]	Exp. [37]
	[MeV]	[fm]	[fm]	[fm]	[fm]
$^{96}Y(0^{-}) \rightarrow ^{96}Zr(0^{+})$	0.973	0.0299	0.7418	0.3920	$\pm 0.8686$
$^{120}\mathrm{Xe}(0^{+}) \rightarrow \ ^{120}\mathrm{I}(0^{-})$	7.309	-0.0114	-0.4565	0.3691	$\pm 0.1967$
$^{140}\mathrm{Ba}(0^{+}) \rightarrow ^{140}\mathrm{La}(0^{-})$	2.109	0.0052	0.1434	0.1142	$\pm 0.1484$
$^{144}\mathrm{Ce}(0^+) \rightarrow \ ^{144}\mathrm{Pr}(0^-)$	1.788	0.0066	-0.1039	0.1355	$\pm 0.0923$
$^{144} Pr(0^-) \rightarrow ^{144} Nd(0^+)$	3.509	-0.0409	-0.2136	0.7617	$\pm 0.2528$
$^{206} \mathrm{Hg}(0^+) \rightarrow ^{206} \mathrm{Tl}(0^-)$	1.912	-0.0199	0.6651	1.3104	$\pm 0.7539$
$^{206}\text{Tl}(0^-) \rightarrow ^{206}\text{Pb}(0^+)$	0.358	0.0217	-0.5811	1.1993	$\pm 0.9873$
$^{210}\text{Pb}(0^+) \rightarrow ^{210}\text{Bi}(0^-)$	1.036	0.0377	0.8331	0.6011	$\pm 0.6751$
$^{212}\text{Pb}(0^+) \rightarrow \ ^{212}\text{Bi}(0^-)$	1.689	0.0358	0.7935	0.8710	$\pm 0.9678$
$^{214}\text{Pb}(0^+) \rightarrow ^{214}\text{Bi}(0^-)$	1.885	0.0383	0.8559	1.0526	$\pm 1.1406$

good agreement with the corresponding experimental data. The calculated matrix elements for the  $^{96}{\rm Y} \rightarrow ^{96}{\rm Zr}$  and  $^{206}{\rm Hg} \rightarrow ^{206}{\rm Tl}$  transitions are closer to the experimental values than the correlated RPA results. The correlated RPA calculations give better results than the present approximation for the  $^{206}{\rm Tl} \rightarrow ^{206}{\rm Pb}$  and  $^{210,212,214}{\rm Pb} \rightarrow ^{210,212,214}{\rm Bi}$  transitions. This case may be attributed to the semi-magic structure of Pb isotopes in which the pairing correlations between nucleons are negligible. The disagreement between the calculated results and the experimental value for the  $^{120}{\rm Xe} \rightarrow ^{120}{\rm I}$  transition may stem from the permanent deformation effects.

# 3.2. Matrix elements for $\Delta J = 2$ transitions

We have performed the calculations for a total of 29 nuclei with the mass range of  $72 \le A \le 204$ . The theoretical and experimental reduced nuclear matrix elements for the unique first-forbidden transitions are shown in Table 3. The first column shows the transitions under consideration. The calculated reduced matrix elements are presented in the third column. The fourth and fifth columns show the other calculated results. The experimental matrix elements, which were extracted from experimental  $\log ft$  values [37], are given in the last column. It can be said that the present approximation is usually successful in reproducing the experimental matrix elements except for a few nuclei. For these nuclei, the inconsistency between the theoretical

and experimental results may be attributed to the permanent deformation effects in nuclear structure. It is significant to reproduce the experimental matrix elements for the U1F transitions due to the effects of these transitions on the total decay probability and the astrophysical processes.

Table 3. A comparison of the calculated reduced matrix elements with the other calculations and the experimental data for  $\Delta J=\pm 2$  transitions. The 2<sup>nd</sup> column shows the calculated energies of the 2<sup>-</sup> states in odd-odd nuclei.

	$\langle J_{\rm f} \mid \mid M(\kappa =$	$1, \lambda = 2, \mu$	$    J_{\rm i} \rangle $ [fm	ո]	
Transition	Energy [MeV]	This work	RPA [2]	pn-QRPA(WS) [11]	Exp. [37]
$^{72}{\rm As}(2^-) \rightarrow ^{72}{\rm Ge}(0^+)$	0.212	-0.1756	0.4254	0.1720	$\pm 0.2029$
$^{82}{\rm Br}(2^{-}) \rightarrow ^{82}{\rm Kr}(0^{+})$	2.423	0.5131	1.9297	0.5287	$\pm 0.5988$
$^{84} Br(2^-) \rightarrow ^{84} Kr(0^+)$	0.373	0.2871	1.3480	0.4404	$\pm 0.3106$
$^{84}\text{Rb}(2^{-}) \rightarrow ^{84}\text{Sr}(0^{+})$	2.541	-0.2547	2.0324	0.5478	$\pm 0.3445$
$^{84}{ m Rb}(2^{-}) \rightarrow ^{84}{ m Kr}(0^{+})$	0.565	-0.3088	1.5500	0.3501	$\pm 0.3036$
$^{86}{ m Rb}(2^{-}) \rightarrow ^{86}{ m Sr}(0^{+})$	1.499	-0.3019	1.4530	0.4552	$\pm 0.3367$
$^{86}{\rm Br}(2^{-}) \rightarrow ^{86}{\rm Kr}(0^{+})$	0.599	0.3236	0.9642	0.4086	$\pm 0.3001$
$^{88}{ m Rb}(2^{-}) \rightarrow ^{88}{ m Sr}(0^{+})$	0.335	0.3742	0.5150	0.4238	$\pm 0.4239$
$^{88}{\rm Kr}(0^+) \rightarrow ^{88}{\rm Rb}(2^-)$	2.530	0.1618	0.0937	0.8365	$\pm 0.1690$
$^{90}{\rm Y}(2^{-}) \rightarrow ^{90}{\rm Zr}(0^{+})$	1.319	0.3876	1.2113	0.5330	$\pm 0.4239$
$^{92}{\rm Y}(2^-) \rightarrow ^{92}{\rm Zr}(0^+)$	0.547	0.3263	1.1722	0.4365	$\pm 0.3938$
$^{94}{\rm Y}(2^{-}) \rightarrow ^{94}{\rm Zr}(0^{+})$	0.014	0.4624	1.0989	0.5136	$\pm 0.3778$
$^{90}{ m Sr}(0^+) \rightarrow ^{90}{ m Y}(2^-)$	2.625	0.1463	0.2395	0.1194	$\pm 0.1506$
$^{92}{\rm Sr}(0^+) \rightarrow ^{92}{\rm Y}(2^-)$	2.647	0.3719	0.3422	0.1788	$\pm 0.5995$
$^{102}\text{Rh}(2^{-}) \rightarrow ^{102}\text{Ru}(0^{+})$	0.494	0.2645	0.4271	0.2111	$\pm 0.5588$
$^{102}\text{Rh}(2^{-}) \rightarrow ^{102}\text{Pd}(0^{+})$	1.320	0.3711	1.0570	0.3438	$\pm 0.2439$
$^{120}I(2^{-}) \rightarrow ^{120}Te(0^{+})$	0.398	0.3091	1.8610	0.3720	$\pm 0.3778$
$^{122}{\rm Sb}(2^-) \rightarrow ^{122}{\rm Sn}(0^+)$	2.158	-0.5947	3.2304	0.6453	$\pm 0.5988$
$^{122}{\rm Sb}(2^-) \rightarrow ^{122}{\rm Te}(0^+)$	3.293	0.2467	1.7336	0.4680	$\pm 0.2674$
$^{124}I(2^{-}) \rightarrow ^{124}Te(0^{+})$	2.479	0.3430	2.7326	0.6150	$\pm 0.3778$
$^{126}I(2^{-}) \rightarrow ^{126}Te(0^{+})$	1.385	-0.6687	3.1254	0.7230	$\pm 0.4594$
$^{132}{\rm La}(2^-) \rightarrow ^{132}{\rm Ba}(0^+)$	1.373	0.2032	2.0986	0.4540	$\pm 0.3001$
$^{136}I(2^{-}) \rightarrow ^{136}Xe(0^{+})$	0.396	-0.1575	2.3621	0.4520	$\pm 0.1487$
$^{140}{\rm Ba}(0^+) \rightarrow ^{140}{\rm La}(2^-)$	2.370	0.2696	0.1944	0.4060	$\pm 0.2936$
$^{142} Pr(2^{-}) \rightarrow ^{142} Nd(0^{+})$	1.063	0.5656	1.4403	0.4600	$\pm 0.5987$
$^{198}{\rm Au}(2^-) \rightarrow ^{198}{\rm Hg}(0^+)$	0.487	-0.0083	0.0777	0.1880	$\pm 0.0119$
$^{198}\text{Tl}(2^{-}) \rightarrow ^{198}\text{Hg}(0^{+})$	0.135	0.1041	1.8409	0.4730	$\pm 0.1893$
$^{204}\mathrm{Au}(2^{-}) \rightarrow ^{204}\mathrm{Hg}(0^{+})$	0.868	0.9562	0.3660	0.6370	$\pm 0.9489$
$^{204}\text{Tl}(2^{-}) \rightarrow ^{204}\text{Pb}(0^{+})$	1.184	0.1235	0.8894	0.3370	$\pm 0.1513$

## 3.3. Log(ft) values for $\Delta J = 0$ and $\Delta J = 2$ transitions

A comparison of the calculated  $\log ft$  values for the first-forbidden  $\Delta J = 0$ ,  $\pm 2$  transitions with the corresponding experimental values is presented in Figs. 1 and 3, respectively. We have performed our Pyatov's restoration calculations based on the shell model calculation, one with a quenching factor and one without a quenching factor. As given in Ref. [2], we have taken  $(g_{\rm A}/g_{\rm V})_{\rm eff}^2 = 0.7(g_{\rm A}/g_{\rm V})^2$  as the quenching factor effect describing the relationship between the effective and free axial weak couplings. In these figures, the \* sign indicates the present results calculated with the quenching fac-

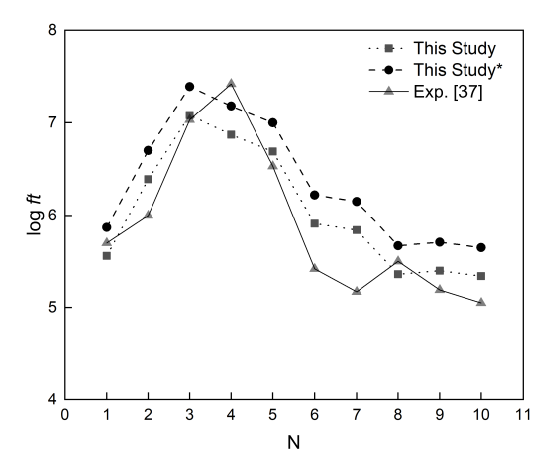


Fig. 1. Calculated and experimental  $\log ft$  values [37] for the first-forbidden  $\Delta J = 0$  transitions. The horizontal axis shows the transitions which are ordered in the same way as in Tables 1 and 2.

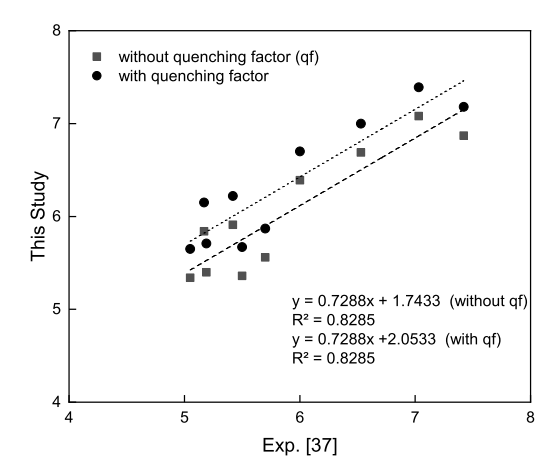


Fig. 2. The R-squared values for the first forbidden  $\Delta J = 0$  transitions.

tor. For  $\Delta J=\pm 2$  transitions, the experimental values usually lie between the theoretical results obtained with and without the quenching factor. In other words, it can be said that the calculated results without the quenching factor can reproduce the experimental data as well as the results calculated with the quenching factor. For  $\Delta J=0$  transitions, the calculated results without quenching factor are closer to the experimental data in comparison with the results obtained with the quenching factor. However, it can be said that the calculated results for  $\Delta J=0$  transitions are not as successful in reproducing the corresponding experimental data as the calculations for  $\Delta J=2$  transitions. For  $\Delta J=0$  transitions, the reason for the deviation of the calculated results from the experimental data can be attributed to the  $\xi$ -approximation used to obtain decay probabilities.

The R-squared values are compiled as the proportion of the variation in the present calculations both without a quenching factor and with a quenching factor that is predictable from the experimental values for the first-forbidden  $\Delta J = 0, \pm 2$  transitions, see Figs. 2 and 4.

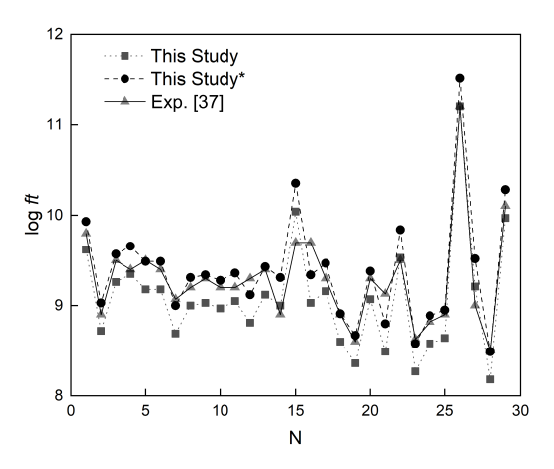


Fig. 3. Calculated and experimental  $\log ft$  values [37] for the first-forbidden  $\Delta J=2$  transitions. The horizontal axis shows the transitions which are ordered in the same way as in Table 3.

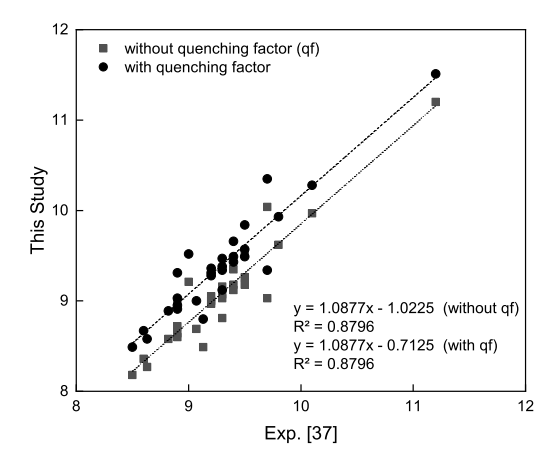


Fig. 4. The R-squared values for the first forbidden  $\Delta J=2$  transitions.

Table 4 shows a comparison of the calculated  $\log ft$  values for a few decays with the shell model results in which a quenching factor was used [38]. For the  $^{96}\mathrm{Y}(0^-) \to ^{96}\mathrm{Zr}(0^+)$  transition, the present result is more successful in reproducing the corresponding experimental data than the shell model calculations. Also, the present calculations need a lower quenching value than q=0.7 in order to reproduce the experimental data related to the  $^{88}\mathrm{Rb}(2^-) \to ^{88}\mathrm{Sr}(0^+)$  transition. However, the projected shell model result for the  $^{94}\mathrm{Y}(2^-) \to ^{94}\mathrm{Zr}(0^+)$  transition shows a better agreement with the corresponding experimental data in comparison with the present result.

Table 4. A comparison of the present  $\log ft$  values with other calculations and experimental data for a few decay transitions.

	Present	Present			
Transition	(without	(with quenching	SM [38]	PSM [38]	$\operatorname{Exp}\left[37\right]$
	quenching)	q = 0.7)			
$^{96}Y(0^{-}) \rightarrow ^{96}Zr(0^{+})$	5.56	5.87	7.90	7.47	5.70
$^{88}{\rm Rb}(2^-) \to ^{88}{\rm Sr}(0^+)$	9.00	9.31	8.87	9.08	9.20
$^{94}{\rm Y}(2^-) \rightarrow \ ^{94}{\rm Zr}(0^+)$	8.81	9.12	9.13	9.34	9.30

## 4. Conclusion

The first-forbidden 0<sup>-</sup> and 2<sup>-</sup> excited states in odd-odd nuclei are obtained being free of the effective interaction strength parameters within the framework of the pn-QRPA formalism. Pvatov's restoration method is used to determine the effective interaction parameters. In this respect, the broken commutator correlation between the total nucleus Hamiltonian and the charge exchange spin-dipole operator is restored. This method was originally introduced to restore the broken Galilean invariance of pairing interaction and then extended to the restoration of broken symmetries. The investigation of the super-allowed Fermi transitions is related to the isospin invariance of nuclear Hamiltonian. The allowed spin-isospin transitions are sensitive to the violations in SU(4) symmetry property. Therefore, the restoration of SU(4) symmetry violations is very important in the definition of Gamow-Teller transition properties. The charge exchange spindipole transitions are affected by the violations in SU(4) symmetry and translational invariance, but there is no exact symmetry that is defined for these transitions. In other words, the restoration of the broken commutator condition for charge-exchange spin-dipole transitions does not mean any symmetry property. However, it should be emphasized that the goal here is not the restoration of any symmetry property, but the definition of the first-forbidden transitions without using any adjustable interaction parameter. The present effective potential is consistent with the phenomenological single-particle basis. Hence, the selected parametrization for the mean-field potential naturally affects the  $\beta$ -decay quantities. Nevertheless, it should be noted that the parameters of the mean-field potential are fixed to determine the single-particle energies and wave functions.

The present calculations are generally successful in reproducing the experimental  $\log ft$  values. However, an effective comparison with the experimental data can be made by removing the kinematical effects from the calculated results. In this respect, the comparison should be made using the nuclear matrix elements. Such a comparison between theory and experiment gives us an opportunity to check the reliability of our wave functions. Thus, the present matrix elements generally show good agreement with the corresponding experimental data.

It is well known that the theoretical description of the unique first-forbidden decay  $(0^+ \leftrightarrow 2^-)$  probabilities for neutron-rich nuclei plays a key role in the study of astrophysical processes. We think that the present results make an important contribution to understanding the  $\beta$ -decay properties of neutron-rich nuclei.

In the present work, we have focused on  $\beta$ -decay matrix elements and  $\log ft$  values. Let us emphasize that we are planning to study the  $\beta$ -decay strength distributions and charge-exchange spin dipole resonance in the near future.

The present work is supported by the Scientific and Technological Research Council of Türkiye (TÜBİTAK) under grant number 121F206.

## REFERENCES

- [1] J. Suhonen, «Calculation of allowed and first-forbidden beta-decay transitions of odd-odd nuclei», *Nucl. Phys. A* **563**, 205 (1993).
- [2] O. Civitarese *et al.*, «Collective effects induced by charge-exchange vibrational modes on  $0^- \to 0^+$  and  $2^- \to 0^+$  first-forbidden  $\beta$ -decay transitions», *Nucl. Phys. A* **453**, 45 (1986).
- [3] H. Homma et al., «Systematic study of nuclear  $\beta$  decay», Phys. Rev. C 54, 2972 (1996).
- [4] I. Kenar, C. Selam, A. Küçükbursa,  $(0^- \to 0^+)$  First Forbidden  $\beta$ -Decay Matrix Elements in Spherical Nuclei», *Math. Comput. Appl.* **10**, 179 (2005).
- [5] J.U. Nabi, S. Stoica, «Unique first-forbidden  $\beta$ -decay rates for neutron-rich nickel isotopes in stellar environment», *Astrophys. Space Sci.* **349**, 843 (2014).
- [6] I.N. Borzov, «Beta-decay rates», Nucl. Phys. A 777, 645 (2006).
- [7] Q. Zhi *et al.*, «Shell-model half-lives including first-forbidden contributions for r-process waiting-point nuclei», *Phys. Rev. C* **87**, 025803 (2013).
- [8] N. Çakmak et al., «The investigation of  $0^+ \leftrightarrow 0^ \beta$  decay in some spherical nuclei», Pramana J. Phys. **74**, 541 (2010).
- [9] T. Suzuki et al.,  $\ll \beta$  decays of isotones with neutron magic number of N=126 and r-process nucleosynthesis», Phys. Rev. C 85, 015802 (2012).
- [10] T. Marketin, L. Huther, G. Martinez-Pinedo, «Large-scale evaluation of  $\beta$ -decay rates of r-process nuclei with the inclusion of first-forbidden transitions», *Phys. Rev. C* **93**, 025805 (2016).
- [11] J.U. Nabi et al., «Unique first-forbidden  $\beta$ -decay transitions in odd-odd and even-even heavy nuclei», Nucl. Phys. A 957, 1 (2017).
- [12] J. Suhonen, «Quenching of the Weak Axial-vector Coupling Strength in  $\beta$  Decays», *Acta Phys. Pol. B* **49**, 237 (2018).
- [13] S. Sharma, P.C. Srivastava. A. Kumar, T. Suzuki, «Shell-model description for the properties of the forbidden  $\beta^-$  decay in the region "northeast" of  $^{208}$ Pb», *Phys. Rev. C* **106**, 024333 (2022).
- [14] I.N. Borzov, «Self-consistent approach to beta decay and delayed neutron emission», *Phys. Atom. Nuclei* **79**, 910 (2016).
- [15] M.T. Mustonen, J. Engel, «Global description of  $\beta^-$  decay in even—even nuclei with the axially-deformed Skyrme finite-amplitude method», *Phys. Rev. C* **93**, 014304 (2016).
- [16] E.M. Ney et al., «Global description of  $\beta^-$  decay with the axially deformed Skyrme finite-amplitude method: Extension to odd-mass and odd-odd nuclei», *Phys. Rev. C* **102**, 034326 (2020).

- [17] N.I. Pyatov, D.I. Salamov, «Conservation laws and collective excitations in nuclei», Nucleonica 22, 127 (1977).
- [18] T. Babacan *et al.*, «The effect of the pairing interaction on the energies of isobar analogue resonances in <sup>112–124</sup>Sb and isospin admixture in <sup>100–124</sup>Sn isotopes», *J. Phys. G: Nucl. Part. Phys.* **30**, 759 (2004).
- [19] A. Küçükbursa *et al.*, «An investigation of the influence of the pairing correlations on the properties of the isobar analog resonances in A = 208 nuclei», Pramana J. Phys. 63, 947 (2004).
- [20] D.I. Salamov *et al.*, «The isospin admixture of the ground state and the properties of the isobar analog resonances in medium and heavy mass nuclei», *Pramana J. Phys.* **66**, 1105 (2006).
- [21] A.E. Çalık, M. Gerçeklioğlu, D.I. Salamov, «Superallowed Fermi Beta Decay and the Unitarity of the Cabibbo–Kobayashi–Maskawa Matrix», Z. Naturforsch. A 64, 865 (2009).
- [22] A.E. Çalık, M. Gerçeklioğlu, D.I. Salamov, «The isospin mixing and the superallowed Fermi beta decay», *Pramana J. Phys.* **79**, 417 (2012).
- [23] A.E. Çalık, M. Gerçeklioğlu, C. Selam, «The influence of pairing correlations on the isospin symmetry breaking corrections of superallowed Fermi beta decays», *Phys. Atom. Nuclei* 76, 549 (2013).
- [24] H.A. Aygör et al., «Deformation effects on isospin mixing and isobar analogue resonance for <sup>74-80</sup>Kr isotopes», Cent. Eur. J. Phys. 12, 490 (2014).
- [25] T. Babacan, D.I. Salamov, A. Küçükbursa, «Gamow–Teller  $1^+$  states in  $^{208}$ Bi», *Phys. Rev. C* **71**, 037303 (2005).
- [26] D.I. Salamov, S. Ünlü, N. Çakmak, «Beta-transition properties for neutron-rich Sn and Te isotopes by Pyatov method», *Pramana — J. Phys.* 69, 369 (2007).
- [27] L. Arısoy, S. Ünlü, «Contributions of the isobar analogue states to the two neutrino double beta decay process», *Nucl. Phys. A* 883, 35 (2012).
- [28] S. Ünlü, N. Çakmak, C. Selam, «The  $2\nu\beta$ – $\beta$ -decay rates within Pyatov's restoration method», *Nucl. Phys. A* **957**, 491 (2017).
- [29] J.J. Cowan, F.K. Thielemann, «R-Process Nucleosynthesis in Supernovae», Phys. Today 57, 10 (2004).
- [30] J.U. Nabi, «Stellar  $\beta^{\pm}$ -decay rates of iron isotopes and its implications in astrophysics», Adv. Space Res. 46, 1191 (2010).
- [31] S. Ünlü et al., «A theoretical description of the first-forbidden  $\beta$ -decay transitions within Pyatov's restoration method», Pramana J. Phys. 97, 121 (2023).
- [32] W. Greiner, J.A. Maruhn, «Nuclear Models», Springer Berlin Heidelberg, Berlin, Heidelberg 1996.
- [33] A.A. Bohr, B.R. Mottelson, "Nuclear Structure", Benjamin, New York, Amsterdam 1969.

- [34] E.K. Warburton, I.S. Towner, B.A. Brown, «First-forbidden  $\beta$  decay: Meson-exchange enhancement of the axial charge at  $A \sim 16$ », *Phys. Rev. C* 49, 824 (1994).
- [35] V.G. Soloviev, «Theory of Complex Nuclei», Pergamon Press, New York 1976.
- [36] P. Möller, J.R. Nix, «Nuclear pairing models», Nucl. Phys. A 536, 20 (1992).
- [37] C.M. Lederer, V.S. Shireley, "Table of Isotopes", Wiley, New York, Amsterdam 1978.
- [38] B.L. Wang, L.J. Wang, «First-forbidden transition of nuclear  $\beta$  decay by projected shell model», *Phys. Lett. B* **850**, 138515 (2024).